

A Convex Hull Approach for the Reliability-based Design Optimization of Nonlinear Transient Dynamic Problems

Samy Missoum^{*¶}, Palaniappan Ramu[§], Raphael T. Haftka[§]

^{*} Aerospace and Mechanical Engineering Department.
The University of Arizona, Tucson, AZ 85741, USA

[§] Department of Mechanical and Aerospace Engineering
The University of Florida, Gainesville, FL 32661 USA

Abstract

Nonlinear transient dynamic problems exhibit structural responses that might be discontinuous due to numerous critical points. The discontinuous behavior hinders classical gradient-based or response surface-based optimization. However, these discontinuities help to classify the system's responses and identify regions of the design space corresponding to distinct dynamic behaviors. In this paper, data mining techniques are employed to group the responses into clusters. The regions of the design space corresponding to the clusters of unwanted behaviors are delimited with convex hulls. This allows an explicit definition of the boundaries of the failure region in terms of the design variables. In addition, the identification of response clusters, within which the responses might be considered continuous, enables the use of traditional response surface approximation for optimization. The proposed approach is applied to the reliability-based design of a tube impacting a rigid wall, which is optimized for a prescribed dynamic behavior.

Keywords: Reliability-based design optimization, nonlinear transient dynamic problems, data mining, discontinuities, convex hull

I. Introduction

Currently, large-scale structural optimization problems can be solved efficiently with commercially available Finite Element software. However, these problems are often limited to linear and simple nonlinear behavior. There are no systematic and efficient methods to perform optimization of highly nonlinear problems such as

[¶] Corresponding author. Email: smissoum@ame.arizona.edu. Tel.: +1 520 626 5226. Fax.: +1 520 621 8191

those encountered in nonlinear transient dynamic problems (e.g., crash). They typically involve many difficulties such as:

- The computational expense associated with repetitive costly finite element analysis (Kurtaran et al., 2002)
- The difficulty in computing the sensitivity, due to the presence of numerical noise and the often encountered convergence uncertainties in explicit dynamic codes.

In view of the aforementioned difficulties, researchers (e.g., Gu.,2001, Yang et al.,2001, Kurtaran et al., 2002, Sobieszczanski-sobieski et al., 2000) have used metamodels and design of experiments (DOE), to optimize (or simply improve) their design, especially for crashworthiness. The metamodel (or response surface) is used to replace the responses extracted from expensive simulations by a simple analytical model. The model, which is a function of the design variables, is built based on sampling points selected from the design space with a chosen design of experiments. In addition, approximation techniques allow the removal of the numerical noise inherent to the computer simulations.

Another key aspect of most highly nonlinear problems is the presence of numerous critical points (limit and bifurcation points). These points are often characterized with drastic changes in the structural behavior. These sharp changes reflect discontinuities in the response (Braibant et al., 2002, Missoum et al., 2004). As a result, the use of traditional gradient-based or response surface approximation techniques becomes difficult, as most approximation methods do not handle discontinuous functions. In addition, the discontinuities can be triggered by very small variations in loading conditions and design imperfections.

However, the discontinuous response can be used as a tool to identify regions of the design space that correspond to specific dynamic behaviors. This is achieved by identifying clusters in the discontinuous response space through data mining techniques. In particular, this allows the identification of clusters

corresponding to “unwanted” behaviors that are considered as failure. The clusters in the response space translate into specific regions in the design space.

The boundaries between these various regions can be distinctly represented using explicit separation functions expressed in terms of the design variables. This allows an analytical definition of the boundaries of a failure domain that corresponds to an infeasible space for optimization. Also, the boundaries serve as limit state for reliability based design. Since the response within each cluster is assumed to be continuous, it is possible to use traditional response surface approximation techniques.

Moreover, as the regions in the design space are associated with various dynamic behaviors, the identification of specific regions permits the designer to specify a particular behavior. This aspect, along with the decomposition of the design space based on a cluster analysis of the responses, is one of the main objectives of this research. In particular, this work addresses the optimization of nonlinear transient dynamic problems that exhibit discontinuous behaviors.

The regions in the design space are separated by so-called decision functions that can be constructed in various ways. The response data classification is achieved through linear or nonlinear decision functions. Missoum et al. (2004) used hyperplanes and ellipsoids for the definition of a failure region for the reliability-based optimization of a nonlinear transient dynamic problem. The example problem included two design variables, so the decision functions were simple straight lines and ellipses. However, due to the fact that the data is generally non-separable, the linear and quadratic separation functions were shown to be over-conservative. That is, the failure region thus defined might contain points corresponding to an acceptable dynamic behavior.

In this paper, an approach is presented where the decision functions are the faces of a convex hull. A convex hull, is the smallest convex set containing a group of points. The faces of the convex hull represent a set of piecewise linear decision functions defined analytically with respect to the design variables. This makes the

convex hull fundamentally distinct from the hyperplanes in Missoum et al. (2004) that were defined over the whole design space. This convex set leads to a more accurate and less conservative assessment of the failure region. It is to be noted that a convex hull is not limited to two dimensions and can be easily extended to several dimensions (Barber et al., 1996).

Another advantage of the convex hull is the straightforward inclusion of uncertainties in the design process. The analytical expressions of the multiple faces that define the boundaries of the convex hull can be considered as limit-state functions. Therefore, the assessment of a probability of failure in the context of reliability-based design optimization (RBDO) can be performed efficiently through, for instance, Monte-Carlo Simulations (Melchers, 1999). Due to the high sensitivity of nonlinear responses to uncertainties, the inclusion of reliability in the optimization process is essential. Probabilistic approaches such as RBDO are proven to address similar situations well. [e.g., Kharmanda et al., 2004, Royset et al., 2003, Koch et al., 2001, Youn et al., 2004]

This paper presents an approach to decompose the design space based on a convex hull. The convex hull is constructed by using the information provided by a clustering technique applied to structural responses. As a demonstrative example, the methodology is applied to the reliability-based design optimization of a tube impacting a rigid wall. The problem is to minimize the weight of the tube so that no global buckling appears with a given probability, while maintaining good energy absorption. The design variables are the length and the thickness of the tube, which is considered as a normal random variable. The reliability index and the absorbed energy are approximated with response surfaces. The optimum results are compared to those obtained based on linear separation functions.

Sections II to IV provide a background on discontinuities, clustering, decision functions, and reliability-based design optimization. Section V discusses the illustrative example. The results are followed by a discussion section and possible avenues for improvement of the proposed method.

II. Discontinuities and clusters

II.1 Discontinuities: a simple example

As an illustrative example exhibiting discontinuities, the classical symmetric shallow two-bar truss (Figure 1) with geometric nonlinearities is used (Crisfield M.A., pp 3-7). The member cross-sectional area is A and the applied force is F . The displacement under the point of application of the force is u . The truss exhibits the typical snap-through behavior as depicted in the force / deflection ($F(u)$) diagram on Figure 2. Two curves are plotted corresponding to trusses with cross sectional areas A and $A + \Delta A$. It can be seen that for the same load F , the system might exhibit snap-through (displacement u_2) or not (displacement u_1). This can happen for infinitesimally small variation ΔA , hence the displacement u is a discontinuous function of A . This might be a serious limitation if traditional techniques for optimal design are considered.

II. 2 Response study and clusters: Two-bar truss

In order to study the behavior of the response further, the design space is sampled. The Latin Hypercube Sampling (LHS) technique (Wang., 2003, Butler., 2001) is used with the following ranges for the two variables:

$$A \in [70, 150 \text{ mm}^2]$$

$$F \in [-700, -400 \text{ N}]$$

The design of experiments is constituted of 404 points. The couples (F, A) used are represented on Figure 3 with the axes scaled based on the maximum values F_{max} and A_{max} .

LHS is a space filling technique that generates points within the domain. However, there might be a lack of information on the boundaries of the sampling space. In order to enhance the quality of the sampling, the four vertices of the design space were also included in the design of experiments.

The corresponding values of the displacements, u , are plotted on Figure 4. As the displacement is discontinuous with respect to the force and the area, two clusters are generated. The cluster that contains the circled dots is associated with a snap-through behavior. Every point in each cluster corresponds to a point in

the design space (Figure 3). The set of points corresponding to the two clusters is represented in Figure 5. The clusters result in two regions in the design space that can be separated, in this case, by a straight line. If we want to optimize the two-bar truss enforcing no snap-through, then the design space is limited to the R region. The function separating the two regions can be used as a constraint for optimization and/or a limit state function if uncertainties are considered.

III. Identification of clusters and definition of decision functions

III.1 Cluster identification

In order to identify the regions of interest in the design space, the clusters created by the discontinuities in the response space need to be identified. Statistical methods are available to find clusters within a cloud of points. This work uses one of the most widely used method, the K-means algorithm (Hartigan J.A., 1979). The basic idea of the method is to minimize the sum of the Euclidean distances of the points of a cluster to its centroid. The number of clusters to be identified is an input parameter, which makes K-means a non-supervised approach.

In the two-bar truss example, the cluster separation as depicted on Figure 4 is obvious. In most cases, the data points are not easily separable, as will be shown in the examples treated in this paper.

III.2 Decision functions

Once the clusters are identified in the response space, the corresponding points in the design space can be isolated to form regions. In order to achieve this, simple geometric entities such as lines and convex hulls can be used that confine the points that belong to a cluster in a simply shaped domain.

III.2.1 Linear decision functions

Linear decision functions such as hyperplanes can be used to define the boundaries of the failure regions in the design space. There are several approaches that can be used to create such hyperplanes through classification techniques. In Missoum et al. (2004), linear decision functions were used for two dimensional

problems. An algorithm based on two parallel lines was presented. Also, the decision functions were extended to the use of quadratic functions (ellipses). An example of the definition of linear decision function in the design space (x, y) of an arbitrary problem is provided in Figure 6. The slopes of the two parallel separation lines $g_{r,1}$ and $g_{r,2}$ is defined by the slope of the line joining the two most distant points A and B. The lines $g_{r,1}$ and $g_{r,2}$ are then defined as being the closest parallel lines enclosing all the unacceptable points. It was shown in Missoum et al (2004) that the use of linear and quadratic decision functions might be too conservative and hence over-estimate the failure region. This work extends the idea by defining the boundaries of the failure region using a convex hull which leads to a less conservative approach by defining more precisely the boundaries of the failure region.

III.2.2 Convex hull decision function

A convex hull of a set of points is the smallest convex set that encompasses all the points. Several methods are available to construct a convex hull. This work uses the “convhulln” function available in Matlab which uses the Qhull program to compute convex hulls in arbitrary dimensions in a provably stable way. Qhull implements the Quickhull algorithm (Barber et al., 1996). An example of definition of convex hull in a design space (x, y) of an arbitrary problem is provided in Figure 7.

IV. Reliability-based design optimization (RBDO)

The general form of an RBDO problem is formulated as follows:

$$\text{Min}_{\mathbf{x}} : f(\mathbf{x})$$

$$\text{Such that: } \mathbf{g}_d(\mathbf{x}) \leq 0$$

$$P_f = P(g_r(\mathbf{x}) \leq 0) \leq P_{f_{target}} \quad (2)$$

with, $\mathbf{x} = \{\mathbf{x}_d, \mathbf{x}_r\}$

where \mathbf{x}_d and \mathbf{x}_r are vectors of deterministic and random design variables respectively. \mathbf{g}_d is a vector of deterministic constraints and g_r is a limit state function. $P(g_r(\mathbf{x}) \leq 0)$ is the probability of failure and $P_{f_{target}}$ is the

maximum allowed or target probability of failure. The limit state function ($g_r(\mathbf{x})=0$) divides the design space into a failure domain ($g_r(\mathbf{x})\leq 0$) and a safe domain ($g_r(\mathbf{x})>0$) and hence serves as a safety criterion.

IV.1 Failure probability computation

Reliability-based design involves the computation of a failure probability as shown in Eq (2). The widely used methods to compute the failure probability are Monte Carlo Simulations (MCS) or moment-based methods such as the First Order Reliability Method (FORM). Here, we use MCS to estimate the failure probability. MCS involves the generation of sample points depending on the statistical distribution of the variables. The sample points that violate the safety criterion are considered failed. The failure probability is computed as:

$$P_f = \frac{\text{num}(g_r(\hat{\mathbf{x}}) \leq 0)}{N} \quad (3)$$

Where, $\hat{\mathbf{x}}$ is the randomly chosen sample point, $\text{num}(g_r(\hat{\mathbf{x}}) \leq 0)$ is the number of samples for which $g_r(\hat{\mathbf{x}}) \leq 0$ and N is the total number of samples.

Another widely used measure of safety is the reliability index. It can be directly computed from the failure probability using the following inverse relationship:

$$\beta = -\Phi^{-1}(P_f) \quad (4)$$

Where, Φ is the standard normal cumulative distribution function and β is the reliability index.

The convex hull presented in Figure 7 represents graphically the boundaries of the failure region. Each facet of the hull can be replaced by explicit equations in terms of the design variables. This allows representing the failure domain with explicit boundaries. Each equation is a limit state equation and a point is considered to be failed if it violates all the limit state functions simultaneously. The notion of violation is defined by assigning an inequality to each facet of the convex hull. When a point belongs to the failure region, all the inequalities have a definite sign. In order to find the sign of each inequality corresponding to failure, the computation of each limit state function at a single point in the convex hull is sufficient. For example, the centroid of the cluster can be chosen. For every realization during MCS, the sign of each inequality is compared to the sign

of the same inequality evaluated at the centroid. If all the signs are identical, then the point belongs to the failure domain. This procedure is summarized in Figure 8.

IV.2 Response surface approximations

MCS often generates numerical noise due to limited sample size. Numerical noise in failure probability or reliability index eventually leads the optimization to converge to a spurious optimum. The accuracy of the MCS is dependent on the number of samples. When the target failure probability is very low and only limited sample size is used to perform MCS, it approximates the failure probability to zero which hinders the sensitivity computations in gradient-based optimization. These difficulties motivate the use of response surface approximations which employ lower order polynomials to approximate the failure probability or safety index in terms of design variables. These response surfaces are termed as design response surface and are widely used by researchers performing RBDO (Sues et al., 1996, Qu et al., 2004).

In the design space, failure probability changes by several orders of magnitude. This steep variation in the failure probability introduces additional challenges in requiring to fit response surfaces of higher order. This increases the computational expense. Alternatively, response surface can be fit to the reliability index as it does not suffer abrupt changes in magnitude. This work uses response surfaces to approximate the reliability index.

The widely used metrics to measure the accuracy of the response surface are the R square and the Relative Maximum Absolute Error (RMAE). R square is used to check the global accuracy while RMAE gives a measure of the maximum local error. The expressions for these measures are given as:

$$R^2 = 1 - \frac{\sum_{i=1}^{N_s} (y_i - \hat{y}_i)^2}{\sum_{i=1}^{N_s} (y_i - \bar{y})^2} \quad (5)$$

$$RMAE = \frac{\max(|y_1 - \hat{y}_1|, |y_2 - \hat{y}_2|, \dots, |y_n - \hat{y}_n|)}{STD} \quad (6)$$

where y_i is the actual response value and \hat{y}_i is the corresponding predicted value. \bar{y} is the mean of the actual response and STD is the standard deviation of the actual response values.

V. Nonlinear transient dynamic example

The proposed approach to define the boundaries of the failure domain is applied to a nonlinear transient dynamic problem.

V.1 Problem description

The problem considered is a tube impacting a rigid wall with a velocity of 15 m/s (Figure 9). The objective of this work is to optimally design the tube so that no global buckling appears. That is, a constraint on the dynamic behavior has to be defined to enforce a crushing of the tube following its axis. The thickness t and the length L of the tube are chosen as design variables.. A fixed rectangular section of height 50 mm and width 40 mm has been used. The analysis is performed with the explicit software ANSYS/LS-DYNA and the simulation time is 40 ms. Four masses of 15 Kg are located at the four corners at the rear of the tube. The tube is meshed with 3600 reduced integration Belytschko-Tsai shell elements.

The tube can deform in various ways after impact onto the rigid wall. Here, the dynamic behavior is divided into two main categories: crushing (deformation along its axis) and global buckling. Two examples of these behaviors are given in Figures 10 and 11.

V.2 Design of experiments

LHS is used to sample the design space. The ranges of the two variable are:

$$L \in [300\text{mm}, 1000 \text{ mm}]$$

$$t \in [1.0 \text{ mm}, 5.0 \text{ mm}]$$

The design of experiments, constituted of 100 points, is depicted in Figure 12. As presented in section II.2, the four vertices of the domain were added to the design of experiments. Therefore, the total number of sampling points is 104

V.3 Deletion of invalid analysis

The reduced integration Belytschko-Tsai shell elements exhibit spurious modes. The work done by artificial forces to overcome these modes is termed as hourglass energy (Belytschko et al., 2004). In order to study the response, FE simulations are performed for the 104 points from the DOE. For each experiment performed, the ratio of hourglass energy over the total energy is stored. If the ratio is higher than 10%, the analysis is considered failed. Out of the 104 experiments, 7 failed this criterion and were not considered.

V.4 Response study and clusters

To detect the design for which global buckling occurs, the absolute values of the maximum transverse displacements $|U_{xmax}|$ and $|U_{ymax}|$ are stored.

The sum $|U_{xmax}| + |U_{ymax}|$ is used as a response that encompasses the buckling in the x and y directions. This quantity should clearly exhibit a discontinuity in the global buckling case compared to the case when there is crushing of the tube.

The response is plotted in a 3D diagram with respect to the values of length and thickness (Figure 13). For a clearer visualization of the response behavior, it is projected on the (response, length) subspace (Figure 14). The points with the highest response value (i.e., sum of displacements) correspond to designs with global buckling. At this stage, one could impose an arbitrary limit on the response to select the points that “seem” without buckling. However, the use of the cluster identification technique (K-means) as described in Section III is a less arbitrary way of selecting the points. When using K-means with two clusters, the clusters identified are represented in Figure 14. The circled dots correspond to points with potential global buckling. The clusters in the response space translate into corresponding sets of failure and acceptable points in the design space as represented in Figure 15.

V.5 Construction of decision functions

Decision functions are constructed in the design space to define the boundaries of the failure domain. Here, the convex hull is used as the decision function. In addition, the linear decision function is studied for comparative purpose. The use of linear decision functions reduces to straight lines in case of a two-dimensional problem such as the tube impacting a rigid wall. Based on the algorithm described in Missoum et al. (2004), the resulting separating functions are depicted in Figure 16. The two corresponding line equations are:

$$g_{r1}(t, L) = -\left(\frac{L}{L_{max}}\right) - 1.016\left(\frac{t}{t_{max}}\right) + 1.474 \leq 0 \quad (7)$$

$$g_{r2}(t, L) = -\left(\frac{L}{L_{max}}\right) - 1.016\left(\frac{t}{t_{max}}\right) + 0.949 \leq 0 \quad (8)$$

Based on the convex hull approach, the boundaries of the failure domain are defined as presented in Figure 17. Comparison of figures 16 and 17 clearly shows that the convex hull provides a much more precise and less conservative definition of the failure domain.

V.6 RBDO problem

The RBDO problem considered consist of finding the length L and the thickness t of the tube so that:

$$\underset{L, t}{Min} \quad : V$$

Such that: $E/E_T \geq 0.99$

$$P_f = P(L, t \in \Omega_f) \leq P_{f_{target}} \quad (9)$$

Where V is the volume, E is the internal (absorbed) energy and E_T is the total energy. Ω_f is the failure domain as defined by equations (7) and (8) or the region enclosed by the convex hull as shown in Figure 17. L and \bar{t} , the mean of thickness t are the design variables. While L is deterministic, t follows a normal distribution with

a mean defined as the current iterate of the optimization process and a standard deviation of $\sigma=0.06 \times t_{max}$ mm. The target failure probability is 10^{-3} . Note that the objective function and the energy constraint are functions of the deterministic length and the mean of the thickness only.

The total energy, as computed by LS-Dyna, is the sum of the strain, kinetic, sliding, and hourglass energies. The two last quantities are usually small in comparison to the two other terms. Therefore, the energy ratio allows quantifying the amount of kinetic energy that has been transformed into strain energy. The energy constraint is important in the field of crashworthiness in order to limit the amount of kinetic energy transmitted to passengers.

The RBDO problem presented in (9) involves the computation of a failure probability to evaluate the probabilistic constraint. Since the boundary of the failure domain is represented analytically, the failure probability can be computed. This section discusses the RBDO performed by using linear decision functions or a convex hull approximating the failure domain.

V.6.1 Approximation of the energy constraint using a quadratic response surface

In order to include the energy ratio as a constraint in the RBDO problem, it is approximated with a response surface that not only removes the numerical noise but also prevents the repetitive calls to costly transient dynamic simulations. The response surface is fitted with second order polynomials.

The response surface chosen is a second order polynomial in the $(L/L_{max}, t/t_{max})$ space and is depicted in Figure 18. The blue dots represent the values of exact energy ratio. The sampling data used to build the response surface are the points that belong to the cluster with no global buckling behavior. Therefore, the points used, cover the entire design space. The metrics providing information on the quality of the approximation are given in Table 1.

V.6.2 Estimation of the probability of failure based on linear decision functions

If linear decision functions are used, the computation of the failure probability is rather simple. Since L is deterministic, the probabilistic problem is one-dimensional, and the failure domain is a segment. This situation is represented in Figure 19 for a given value L_0 of L and scaled thicknesses t_1 and t_2 that limit the failure domain. In this case, the failure probability can be expressed analytically as:

$$P_f = \Phi\left(\frac{t_2 - \bar{t}}{\sigma}\right) - \Phi\left(\frac{t_1 - \bar{t}}{\sigma}\right) \quad (10)$$

where, Φ is the standard normal cumulative function.

V.6.3 Estimation of the probability of failure based on the convex hull

In the case where the boundaries of the failure domain are approximated by the facets of the convex hull, MCS is used to estimate the failure probability. As discussed in section IV.1, the facets of the convex hull are replaced by inequalities and the sample points that violate all the inequalities are considered to be failed. Based on this, the failure probability is computed from (3). The number of samples used is 10^6 . Note that in the special case of a two-dimensional convex hull, the probability of failure could be calculated using (10), however, for the sake of generality (higher dimensions and nonlinear decision functions), Monte Carlo simulations are used.

As explained in IV.2, it is recommended to approximate the reliability index instead of the probability of failure directly. A second order polynomial in terms of L/L_{max} and t/t_{max} is used and is presented in Figure 20. The blue dots are the values of the actual reliability index. The approximated surface for the reliability index seems to represent the actual value well in the central part of the design space. A more precise description of the accuracy is given by the error statistics in Table 1.

V.6.4 Results

The approximated reliability index and the energy ratio can now be used to solve the optimization problem defined in (9). Note that the energy ratio response surface is identical for the linear and convex hull cases. The results are presented in Table 2 with a target probability $P_{f,target} = 1.0 \times 10^{-3}$ (reliability index of 3.090). In both cases the energy and the probability of failure constraints are considered active.

For the convex hull approach, the transient dynamic simulation was run for the optimal values of the design variables presented in Table 2. It was observed that the energy ratio value of 0.999 computed from the simulation was accurately approximated by the response surface as 0.99. It can be observed that there is an error of 1% in the energy ratio response surface. The corresponding actual value of the probability of failure at the optimum is estimated using equation 10 and Monte Carlo simulation as 0.001342 and 0.0014 respectively. This indicates that the obtained final design in both cases is less conservative than the target design. The relative errors between the approximated and the actual values of the probability of failure, reliability index for the two cases are gathered in Table 3.

The error on the predicted reliability is of course dependent on the quality of the response surface approximation. However, it is also important to quantify the variability of the calculated probabilities at the points used for the construction of the response surface. In the case of MCS, the probability of failure based on 10^6 samples varies from one run to another. These variations can be quantified using the following relation which provides the standard deviation σ of the estimated probability of failure:

$$\sigma = \sqrt{\frac{P_f(1-P_f)}{N}} \quad (11)$$

where P_f and N are the probability of failure and the number of samples respectively. The MCS is subjected to an error of $N_f^{-\frac{1}{2}}$ where N_f is the number of failed samples. In this case, the error is close to 3% which is indeed confirmed by the relative error of reliability index in Table 3. The 3% error in reliability index is translated as 40% error in the failure probability.

Also, note that in the course of optimization based on the convex hull, it was observed that the optimization algorithm converged to different optimal designs for different starting points. In an attempt to understand this, the optimization problem stated in (9) was treated graphically and presented in Figure 21. The constraints are represented by dashed lines with a shaded feasible domain. The contours of the objective function are presented in the solid lines.

The optimal solution is such that both constraints are active. It can be noted that there are two local minima, and the results reported in Table 2 corresponds to the better of the two.

It can be clearly observed that the optimal design obtained using a convex hull presented in Table 2 is lighter than the design obtained using linear decision functions. This is due to the fact that the probabilistic constraint pushes the design away from the boundaries of the failure domain that is already somewhat conservative compared to the convex hull.

VI. Discussion

In the nonlinear transient dynamic example discussed in this paper, the convex hull approach seems to define the boundaries of the failure region more accurately than the two line separation functions. However, this is valid only around the optimum found. In fact, parts of the actual failure region might not be represented by the convex hull. The most stringent example of this phenomenon is given by the two bar truss. The convex hull defining the boundaries of the failure region for the two bar truss is presented in Figure 22. In this case, the failure region is actually a half plane bounded by a single line as represented in Figure 5. However, it can be observed in Figure 22 that the convex hull leaves the region above the topmost facet as safe whereas failure occurs in this region. Moreover, the facets of the convex hull which are common to the boundaries of the sampling space are artificial. Hence, the area of the failure region may be highly underestimated. For example, inspection of figure 22 shows that a reduction of the area ratio to 0.4 would lead to a safe design. Clearly this is not possible as the design would buckle for such an area. This example shows how the bounds on the design variables might dictate the geometry of the convex hull.

For the impact problem, investigation of the region above the facet formed by endpoints (16, 30) of Figure 17 shows that parts of the failure regions might also be missed. The reason for this is that the convex hull is constructed based only on the sampling points. As the set of sampling points is fixed, no other information is provided. Hence, the definition of the failure domain by the convex hull is very dependent on the initial design of experiments. For this particular problem, the bounds on the design variables do not artificially limit the failure domain because of the location of the optimum and the fact that the length is deterministic.

In order to minimize the impact of these difficulties and to improve the use of the convex hull approach, the following improvements could be investigated:

- A solution to reduce the error in the definition of the failure region would be to remove some of the inequalities defining the convex hull which are artifacts of the fixed design of experiments. Despite the fact that for two dimensional cases, the physics of the problem and a graphical inspection might help to decide which inequality should be dropped, the procedure discussed in the appendix, extendable to higher dimensions, can be employed to identify the artificial facets of the convex hull.
- Since the convex hull is based on the samples generated by the DOE, it is recommended to use a space filling technique in which the samples are spaced as uniformly as possible. For instance, the Optimal Latin Hypercube Sampling (OLHS) where the minimum distance between points is maximized can be used (Butler, 2001). However, this improves the distributions of sample points inside the domain and special care should be taken for the boundaries. In this paper, the vertices of the domain were added, but other points on the boundaries could be added to the design of experiments.

VII. Conclusion

A convex hull approach to handle discontinuous response in nonlinear structural problems is proposed. The method consists of identifying regions of the design space that encompasses points corresponding to

unwanted behaviors. These points are obtained through the identification of response clusters originating from discontinuous behaviors. The boundaries of the failure region are defined explicitly based on a convex hull.

The explicit knowledge of the failure domain can be used for reliability-based optimization. The facets of the convex hull are transformed into explicit limit state inequalities that must be violated simultaneously for failure to occur. Based on Monte Carlo Simulations, this allows an efficient calculation of the failure probability. The proposed method, which allows the prescription of a given mechanical behavior, is applied to the optimal design of a tube impacting a rigid wall.

The next stages of this research involve the improvement of the techniques used for the definition of the failure region for two and three dimensional problems. Also, the methodology should be applied to other types of uncertainties such as material properties, loads and presence of defects.

Acknowledgments

The authors would like to acknowledge the partial funding from Pôle Universitaire Léonard de Vinci, France, in a collaborative research effort with the University of Florida.

Appendix

Identifying the suspicious facets:

Method 1:

- 1) For every point in the design space, evaluate all the inequalities of the convex hull

- 2) If there exist a facet such that no point satisfies it while violating all the other facets, then this particular facet is suspicious as it might be artificial. In the impact problem, it is the case for the facets with end points (16, 30) and (27, 25). Note that facets (3, 9), (9, 15) and (15, 27) also fall into this category.

This method is a conservative approach to identify the suspicious facets. In case of a convex hull with small convexity, the facets are almost aligned and are likely to be flagged as suspects even with points rather close to a facet. Instead, the method can be slightly modified as follows:

Method 2:

- 1) For all the points lying outside the convex hull in the design space, compute the perpendicular distance to the facets of the convex hull.

- 2) If there exist a facet such that no point's projection (shortest distance) is on the facet considered, then it is suspicious. For the transient dynamic problem, this procedure will only flag facets with end points (25,27), (30,16) as suspicious.

It is noteworthy that the artificial facets lying on the boundaries of the design space would be automatically flagged as suspicious with any of the two approaches.

Generating Test Points and checking for artifacts:

Once the suspicious facets are identified using either of the above methods, test points that are samples satisfying the suspicious facets can then be generated. For example, for a two dimensional problem, it could be generated at the centre of the candidate facet at an eccentricity away from the convex hull (Figure 23). The test point can be chosen at a small distance (function of the facet's main dimension) from the facet on the outwards normal at the middle of the facet.

This sample is tested for its response. If it fails, the facet is an artificial facet and the corresponding inequality can be removed from the approximation of the failure region. If the response corresponding to the generated sample exhibits acceptable behavior, then the facet is a natural facet of the convex hull.

Based on the test point results, the convex hull can be updated. The suspicious facet identification technique followed by the test point check can then be repeated iteratively until convergence.

References

Barber, C. B., D. P. Dobkin, and H. T. Huhdanpaa (1996). The quickhull algorithm for convex hulls. *ACM Transactions on Mathematical Software* 22(4), 469-483.

Braibant, V., M. Bulik, M. Liefvendahl, S. Molinier, R. Stocki, and C. Wauquiez (2002, 25-27 November). Stochastic simulation of highly nonlinear dynamic systems using the M-Xplore extension of the RADIOSS software. In *Proceedings of the Workshop on Optimal Design*, Laboratoire De Mécanique Des Solides, Ecole Polytechnique 91128 Palaiseau.

Butler, A. N. (2001). Optimal and orthogonal latin hypercube designs for computer experiments. *Biometrika* 88(3), 847-857.

Crisfield, M. A. (1994). Non-linear finite element analysis of solids and structures. Volume 1. John Wiley and Sons.

Gu, L. (2001, 9-12 September). A comparison of polynomial based regression models in vehicle safety analysis. In *ASME Design Engineering Technical Conferences – Design Automation Conference (DAC)*, Pittsburgh, PA, ASME, Paper No. DETC2001/DAC-21063.

Hartigan, J.A. and M. A. Wong (1979) Algorithm AS 136: A K-means clustering algorithm. *Applied Statistics* 28, 100-108.

Kharmanda, G., A. Mohamed, and M. Lemaire (2002). Efficient reliability-based design optimization using a hybrid space with application to finite element analysis. *Structural and Multidisciplinary Optimization* 24, 233-245.

Koch, P. N. and L. Gu (2001, 18-19 June). Addressing uncertainty using the Isight probabilistic design environment. In *First Annual Probabilistic Methods Conference*, Newport Beach, CA.

Kutaran, H., A. Eskandarian, D. Marzougui, and N. E. Bedewi (2002). Crashworthiness design optimization using successive response surface approximations. *Computational Mechanics* 29, 409-421.

Madsen, H. O., S. Krenk, and N. C. Lind (1986). *Methods of structural safety*, Prentice-Hall, Englewood Cliffs, NJ.

Melchers, R. E., *Structural Reliability Analysis and Prediction*, Wiley, New York, 1999

Missoum, S., S. Benchaabane, and B. Sudret (2004, 19-22 April). Handling bifurcations in the optimal design of transient dynamic problems. In *45th AIAA/ASME/ASC/AHS/ASC Structures, Structural Dynamics & Materials Conference*, Palm Springs, CA.

Qu, X. and R. T. Haftka (2004). Reliability-based design optimization using probabilistic sufficiency factor. Paper accepted for publication by *Journal of Structural and Multidisciplinary Optimization*

Royset, J.O., A. D. Kiureghian, and E. Polak (2003). Successive approximations for the solution of optimal design problems with probabilistic objective and constraints. In Der Kiureghian, Madanat and Pestana (Eds.), *Applications of Statistics and Probability in Civil Engineering*, pp.1049-1056, Millpress, Rotterdam, ISBN 90 5966 004 8.

Sobieszczanski-Sobieski, J., S. Kodiyalam, and R. J. Yang (2001). Optimization of car body under constraints of noise, vibration, and harshness (NVH), and Crash. *Structural and Multidisciplinary Optimization* 22(4), 295-306.

Sudret, B. and A. D. Kiureghian (2000). Stochastic finite element methods and reliability. A state-of-the-art report. Report No. UCB/SEMM-2000/08. Department of Civil and Environmental Engineering. University of California, Berkeley.

Sues, R. H., D. R. Oakley and G. S. Rhodes (1996). Portable parallel computing for multidisciplinary stochastic optimization of aeropulsion components. Final Report, NASA Contract NAS3-27288

Ted Belytschko., Wing Kam Liu and Brian Moran., *Nonlinear Finite Elements for Continua and Structures*, John Wiley and Sons, 2004

Wang, G. G. (2003). Adaptive response surface method using inherited latin hypercube design points. *Transactions of the ASME, Journal of Mechanical Design* 125, 210-220.

Yang, R.J., N. Wang, C. H. Tho, and J. P. Bobineau (2001, 9-12 September). Metamodeling development for vehicle frontal impact simulation. In *ASME Design Engineering Technical Conferences – Design Automation Conference (DAC)*, Pittsburgh, PA, ASME, Paper No. DETC2001/DAC-21012.

Youn, B. D., K. K. Choi, R. J. Yang, and L. Gu (2004). Reliability-based design optimization for crashworthiness of vehicle side impact. *Structural and Multidisciplinary Optimization* 26, 272-283.

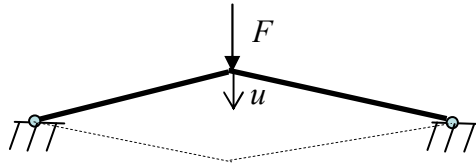


Figure 1. Symmetric two-bar truss

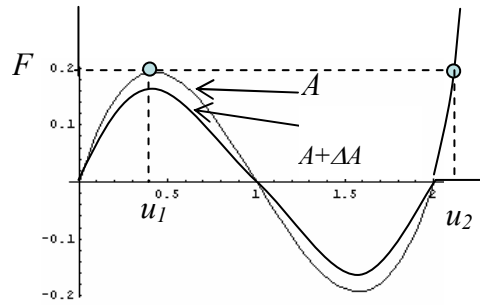


Figure 2. Force – deflection diagram. Two-bar truss. Snap-through occurs for a small variation ΔA of the cross-sectional area A .

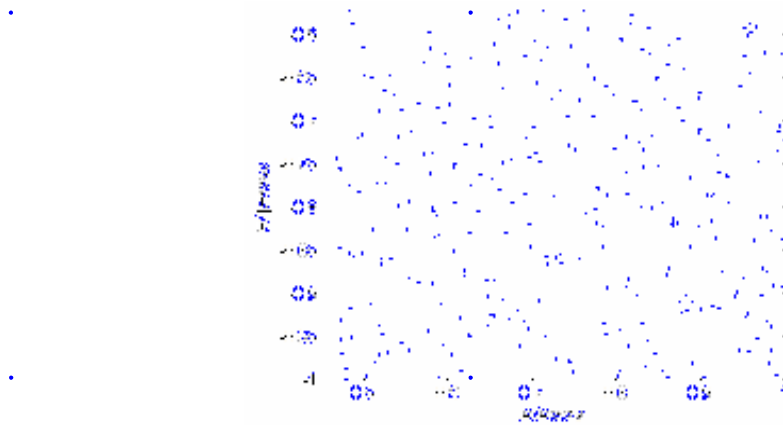


Figure 3. LHS design of experiments for the two bar truss problem. 404 points. Variables: area(A) and force(F).

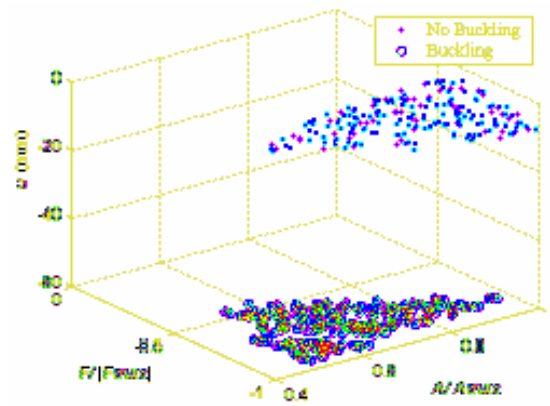


Figure 4. Displacement u with respect to force and area for the two bar truss problem. Two clusters corresponding to stable and buckling behaviors.

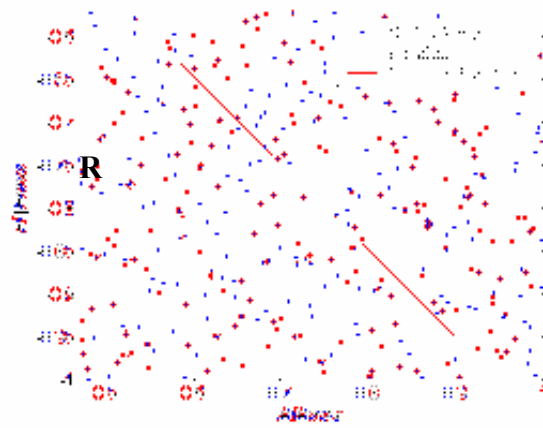


Figure 5. Decomposition of the two bar truss design space into two regions. The R region corresponds to a stable behavior.

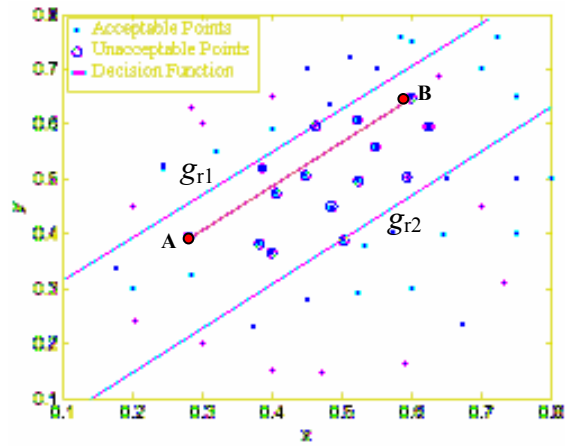


Figure 6. Example of linear decision functions in a design space (x, y) , based on the algorithm in Missoum et al. (2004).

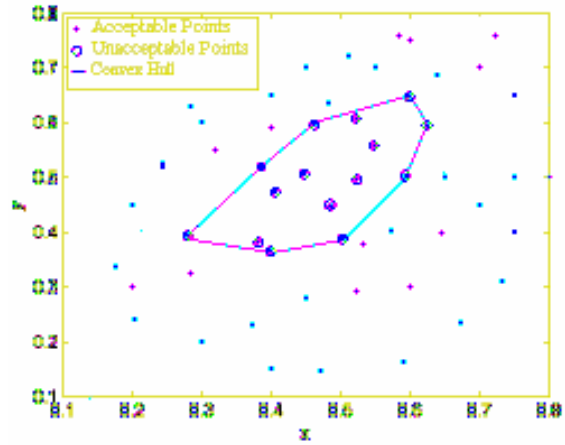


Figure 7: Example of convex hull in a design space (x, y)

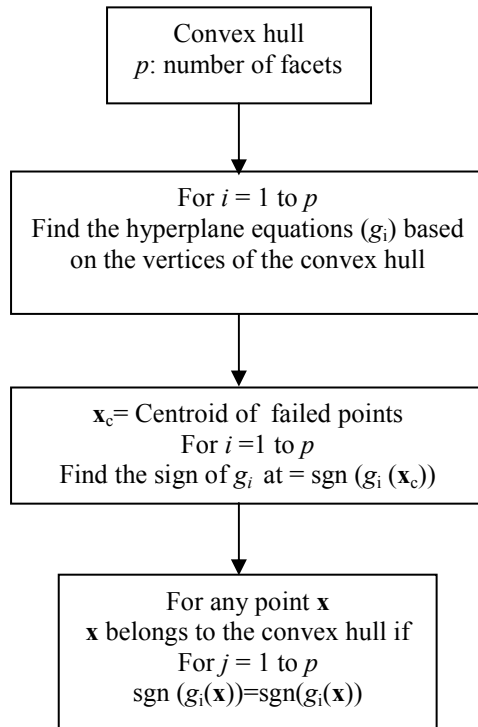


Figure 8. Procedure to identify points belonging to the failure region defined by convex hull

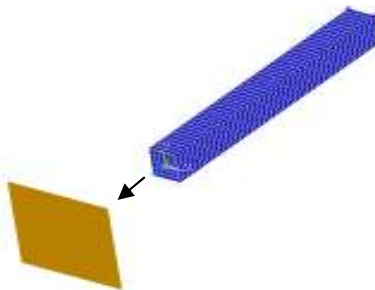


Figure 9. Tube impacting a rigid wall.

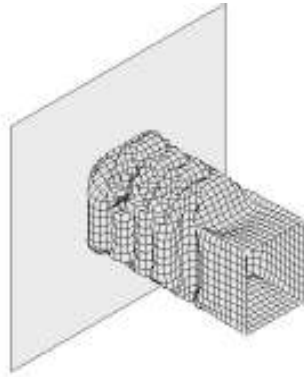


Figure 10. Crushing of the tube

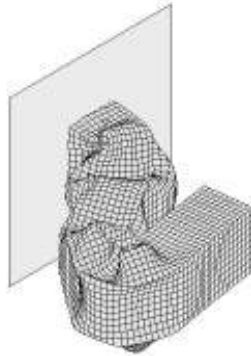


Figure 11. Global buckling of the tube

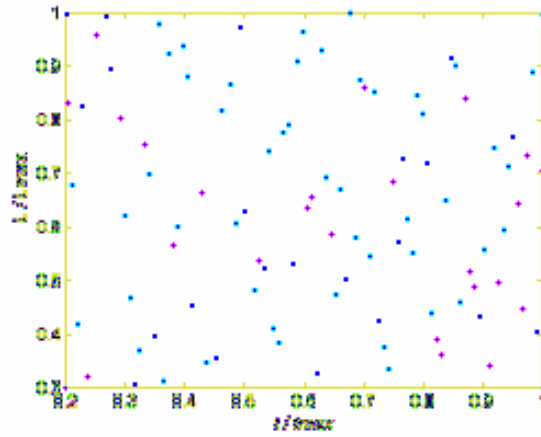


Figure 12. LHS design of experiments for the transient dynamic problem. The vertices of the design space are added. 104 points

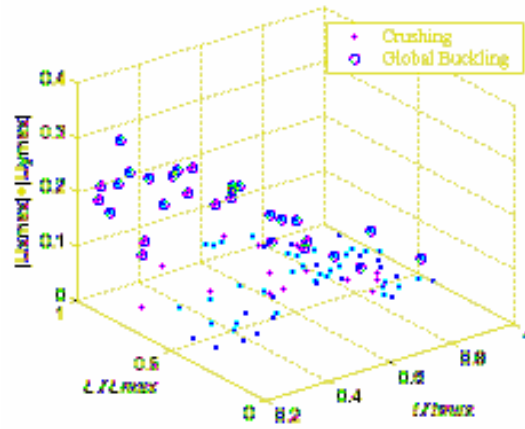


Figure 13. Response plot (sum of the absolute transverse displacements) with respect to the length and thickness for the transient dynamic problem

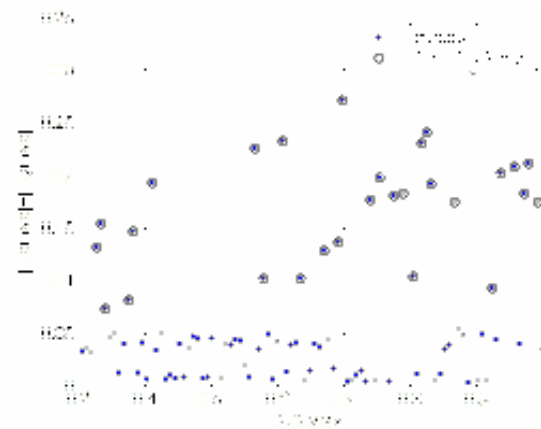


Figure 14. Response projected on the (response, length) subspace. Transient dynamic problem.

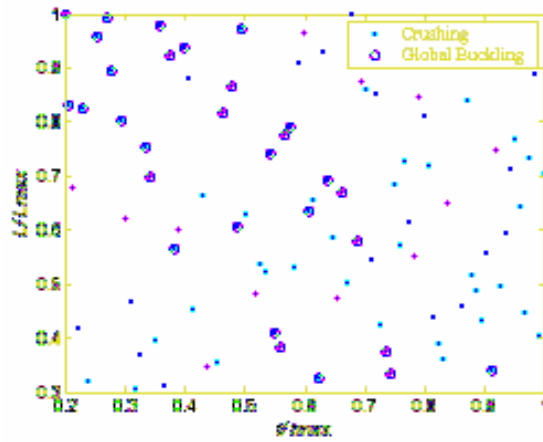


Figure 15. Distribution of failure and acceptable points in the design space (length, thickness) for the transient dynamic problem

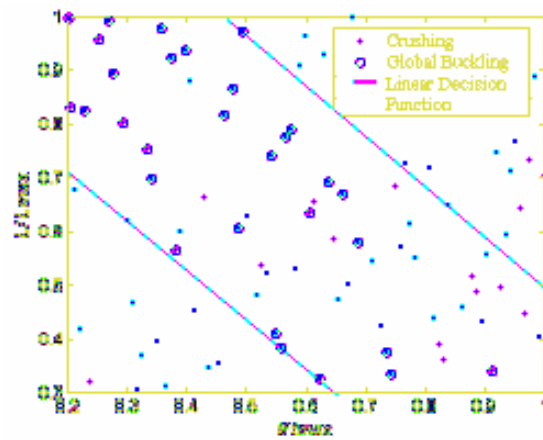


Figure 16. Linear decision functions used to define the failure domain for the nonlinear transient dynamic problem. Approach used in Missoum et al (2004).

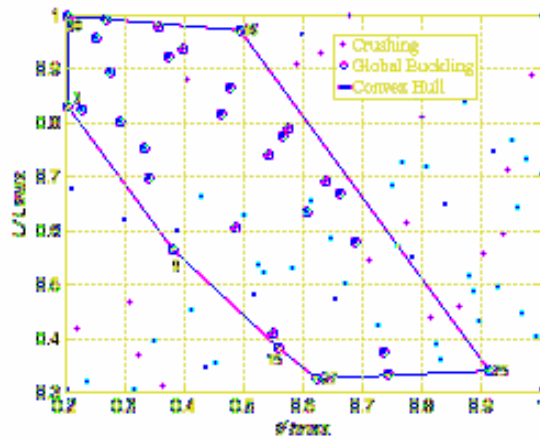


Figure 17. Convex hull used to define the failure domain for the nonlinear transient dynamic problem

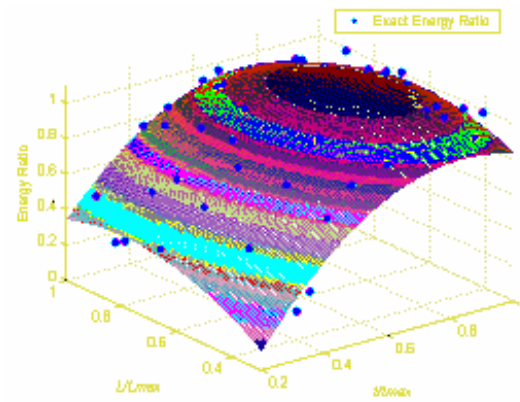


Figure 18. Response surface of approximated energy ratio with respect to thickness and length.

Failure points are excluded from the approximation.

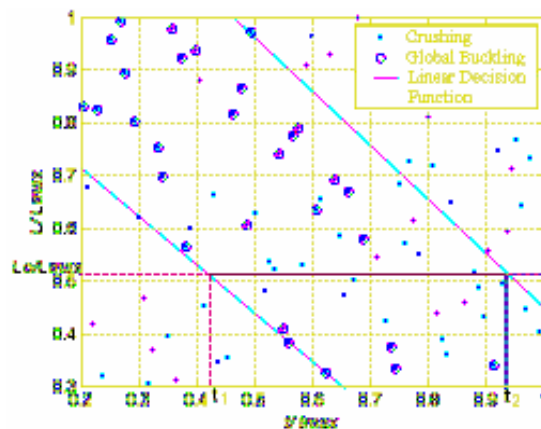


Figure 19. Failure domain (thick line) when t is the random variable. Linear decision functions from Missoum et al. (2004).

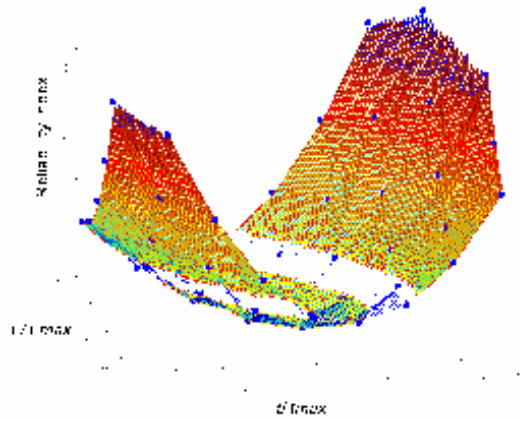


Figure 20. Response surface for the reliability index. Failure domain delimited using the convex hull.

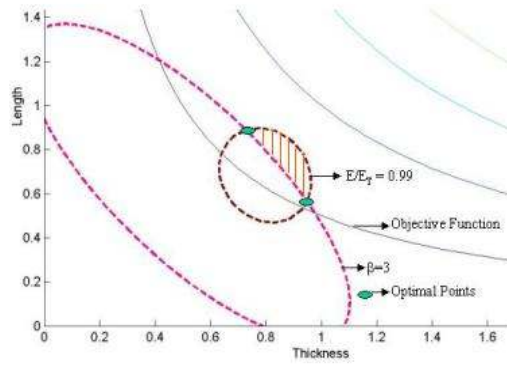


Figure 21. Graphical representation of the RBDO problem using the convex hull approach.

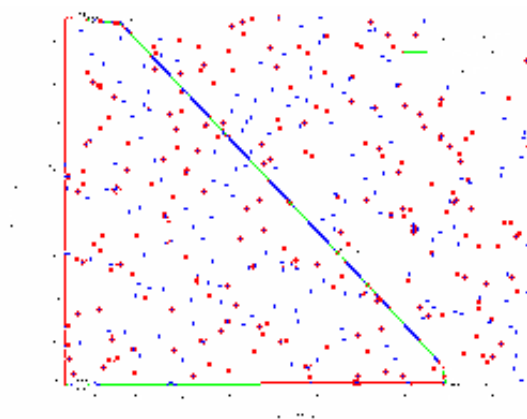


Figure 22. Two bar truss. Failure region approximated by a convex hull.



Figure 23. Example of test point generated to check whether a suspicious inequality is to be removed.

Transient dynamic problem.

Table 1: Error metrics for the response surfaces.

See Eqs. (5) and (6) for definition of metrics.

Metrics	Reliability index	Energy ratio
R^2 (Eq. 5)	0.8524	0.8992
RMAE(Eq. 6)	1.03	0.7639

Table 2. Optimal design for the transient dynamic problem –Comparison between linear separation

function and convex hull

	Optimum		
	\bar{t}/t_{max}	L/L_{max}	$V(\text{mm}^3)$
Convex hull	0.948	0.558	423014.5
Linear	0.98	0.665	522024.7

Table 3. Relative errors between predicted and actual probability of failure, reliability index estimated from Eq 10 and MCS (1e6 samples). Convex Hull.

Method	Probability	Reliability Index
Response Surface	0.001	3.0902
Actual (Eq. 10)	0.001342	3.00169
Relative Error (%)	34.2	2.9
Actual (MCS)	0.0014	2.9924
Relative Error (%)	40	3.2